

Zero-Shear Viscosity Properties of Solutions of Flexible Polymers in Light of Renormalization Group Theories

Bo Nyström

Department of Chemistry, The University of Oslo, P.O. Box 1033, Blindern N-0315, Oslo 3, Norway

Received October 19, 1992; Revised Manuscript Received March 26, 1993

ABSTRACT: The zero-shear viscosity behavior, in the dilute and semidilute regimes, in solutions of polystyrene under good and Θ solvent conditions, is analyzed in the framework of a recent theoretical model due to Shiwa. At good solvent conditions, this model, which takes into account the gradual screening of both hydrodynamic and excluded-volume interactions as well as entanglement constraints, is consistent with the large amount of experimental data collected from the literature. In the course of this study the behavior of the radius of gyration as a function of an experimentally accessible reduced concentration variable is tested against experimental results. A reasonably good agreement is found. In the analysis of the universal viscosity properties, it is argued for the use of the reduced dynamic scaling variable $c[\eta]$ in lieu of the static counterpart c/c^* . At the Θ state the viscosity features are observed to be more complex.

Introduction

In recent years renormalization group (RG) theories and related approaches have constituted a powerful tool in the description of universal static¹⁻⁸ and dynamic⁹⁻¹⁴ features of flexible polymers in solution. The concentration region explored in these studies ranges from the dilute domain to the "effective" semidilute regime, where the polymer coils strongly overlap each other but still occupy a small volume fraction Φ of polymer ($\Phi < 0.2$).

In the theoretical models advanced by Shiwa et al.^{10,11} for the description of the universal crossover behavior (i.e., the overlap-parameter dependence) of collective transport phenomena, such as sedimentation velocity and translational diffusion of polymers at concentrations not extending beyond the effective semidilute regime at good solvent conditions, the effects of the gradual screening of both hydrodynamic and excluded-volume interactions have been taken into account. The importance of these effects have been endorsed by recent studies, where experimental sedimentation^{15,16} and diffusion^{17,18} data have been analyzed in the framework of these models. For cooperative diffusion as well as for sedimentation in the semidilute regime, the entanglement of chains should not be important, because all the chains are more or less collectively moving.

In contrast to these collective processes, transport phenomena such as self-diffusion, tracer diffusion, and viscosity are all closely associated with the motion of individual chains; hence, entanglements are expected to play a crucial role. In a previous theoretical study,¹⁰ on the concentration and molecular weight dependence of the self-diffusion coefficient of polymer solutions in the dilute and the semidilute regimes, a formalism, based on the microscopic model of Hess¹⁹ combined with RG calculations, was developed in order to take into account the effect of the entanglement constraint on chain dynamics. The potential of this approach has further been elucidated in an investigation,²⁰ where a large body of self-diffusion and tracer diffusion data was compared with the theoretical predictions. These studies strongly support the hypothesis that entanglements produce strong topological restrictions on the mobility of the individual polymer chains.

In the literature only a few theoretical models, based on RG ideas, have been elaborated to describe the crossover behavior of the zero-shear viscosity or related quantities

of polymer solutions. By combining a mode-mode coupling theoretical approach and RG results, Shiwa et al.¹¹ accounted for the progressive screening of both hydrodynamic and excluded-volume interactions in the description of the crossover behavior of viscosity-related properties in dilute and semidilute polymer solutions. By using pure RG methods, Stepanow and Helmis²¹ considered the effects of the excluded-volume and hydrodynamic interactions on the zero-shear viscosity of polymer solutions. However, these models both suffer from a common inherent weakness; namely, the effect of entanglement constraints has not been taken into account. This deficiency of the theories is clearly revealed when the theoretical predictions are compared with experimental viscosity results. It was observed^{11,21} that the deviation between the theoretical functions and the experimental data became progressively more pronounced as the degree of chain overlapping increased. However, quite recently Shiwa²² devised a procedure in the framework of RG calculations, together with a mode-coupling method to include the gradual screening of both hydrodynamic and excluded-volume interactions as well as the effect of entanglements. This latter effect was incorporated with the aid of the approach of Hess.¹⁹

It is the aim of this study to examine the universal features of the reduced zero-shear polymer viscosity and related quantities and to survey the quantitative importance of entanglement effects in this type of transport process. For this purpose a large amount of experimental data on zero-shear viscosity in solutions of polystyrene at good and Θ solvent conditions, over a wide concentration range ($\phi \leq 0.2$), has been collected. In the analysis of the results we will, to a large extent, resort to the theoretical model of Shiwa.²² This approach will be outlined below, and inherent shortcomings associated with this model will be discussed.

In the course of the presentation of the results, theoretical predictions of static quantities, relevant for the viscosity models, will be compared with experimental results. In the examination of universal viscosity properties, the advantages of using a reduced dynamic scaling variable in lieu of a static variable will be elucidated. In addition to the analysis of the viscosity data at good solvent conditions, some features associated with the viscosity behavior at Θ solvent conditions will be scrutinized.

Theoretical Considerations

At low, but finite, concentrations the zero-shear polymer solution viscosity η is frequently expressed by the following empirical expansion form:

$$\eta = \eta_0(1 + [\eta]c + k_H[\eta]^2c^2 + \dots) \quad (1)$$

where η_0 is the viscosity of the pure solvent, $[\eta]$ is the polymer intrinsic viscosity, c is the polymer mass concentration (mass/volume), and k_H is the dimensionless Huggins coefficient, which characterizes the first-order effects of interaction on the zero-shear viscosity. Usually the viscous properties of dilute and semidilute polymer solutions are analyzed in terms of the dimensionless reduced zero-shear polymer viscosity, which can be expressed by the expansion form

$$\eta_R \equiv \eta_{sp}/c[\eta] = 1 + k_H c[\eta] + \dots \quad (2)$$

in which $\eta_{sp} = (\eta - \eta_0)/\eta_0$. It has previously been demonstrated²³⁻²⁷ that a plot of η_R versus $c[\eta]$ practically condenses viscosity data onto a master curve. In recent papers²⁵⁻²⁷ eq 2 is often cast into the following form:

$$\eta_R = 1 + k(c/c^*) + \dots \quad (2a)$$

where c^* denotes the critical concentration at which polymer coils begin to overlap and is frequently defined as

$$c^* = \frac{3M}{4\pi R_{G,0}^3 N_A} \quad (3)$$

Here M is the molar mass of the solute, $R_{G,0}$ is the radius of gyration of the isolated polymer, and N_A is Avogadro's constant. By using the Flory-Fox equation, $[\eta] = 6^{3/2} \Psi R_{G,0}^3/M$ where Ψ (mol⁻¹) is the Flory viscosity factor, the parameter k in eq 2a may be expressed as

$$k = \frac{(3)(6^{3/2})k_H\Psi}{4\pi N_A} \quad (4)$$

A few years ago Shiwa et al.¹¹ (the S-O-B theory) devised a theoretical approach for the analysis of crossover behavior of the polymer viscosity. In this model the gradual hydrodynamic screening effect is incorporated with the aid of a mode-coupling scheme and the gradual screening of excluded-volume interactions is considered on the basis of the RG method. In the framework of this model the change of the polymer solution viscosity with increasing coil overlap may be written in the form^{11,28}

$$(\eta/\eta_0)_{S-O-B} = 1 + \alpha r \kappa^2 \quad (5)$$

with²

$$\alpha = (1/6)(1 - 31\epsilon/96 + \gamma\epsilon/8) \quad (5a)$$

where $r \equiv R_{G,c}^2/R_{G,0}^2$ and κ , the inverse of the reduced hydrodynamic screening length, are both functions of the overlap parameter X . Here we may consider $R_{G,0}$ as the radius of gyration of a "test" chain at infinite dilution and $R_{G,c}$ is its value in a solution of identical chains of concentration c . Equation 5a is derived in the framework of the ϵ -expansion method, where $\epsilon = 4-d$, d being the dimensionality. The quantity $\gamma \approx 0.5772$ is Euler's constant.

At Θ solvent conditions (Gaussian chains) the quantity κ is given by

$$X = (4/3)(-\pi^{1/2}) + (\pi/2)(\kappa + \kappa^{-1}) - (\pi/2\kappa) \exp(\kappa^2)(1 - \text{erf}(\kappa)) \quad (6)$$

where the error function $\text{erf}(\kappa) = (2/\pi^{1/2}) \int_0^\kappa \exp(-t^2) dt$.

At good solvent conditions (excluded-volume interactions) no simple analytical expression is available for the determination of κ , but the coupled equations may be solved numerically, yielding values of κ as a function of X . The values of κ may also be read off from the graph of κ versus X , depicted in the original paper.¹¹

Experimentally it is well established²⁹⁻³² that the radius of gyration of a test chain, immersed in a semidilute solution of other identical polymer chains, shrinks as the matrix concentration increases. Some years ago Ohta and Oono^{1,4} developed in the framework of the conformation space RG formalism, together with the ϵ -expansion method up to order $\epsilon = 4-d$, an explicit functional form of r as a function of X . In the case of a monodisperse polymer, a relationship of the following form emerges:⁴

$$r = \exp\left(\frac{\epsilon}{4} X G(z)\right) \quad (7)$$

where

$$z = 2(1 + X) \quad (8)$$

and the function $G(z)$ is given by

$$G(z) = 3/z + \frac{1}{2} \exp(z) \text{Ei}(-z) \left(1 - \frac{4}{z} + \frac{6}{z^2}\right) - \left(\frac{1}{z} + \frac{3}{z^2}\right)(\gamma + \ln(z)) \quad (9)$$

where $\text{Ei}(-z) = -\int_z^\infty dt e^{-t}/t$.

By using a slightly different renormalization scheme, Ohta and Nakanishi² arrived at the following expression:

$$r = \exp\left(-\frac{\epsilon}{4} \int_0^\infty y^5 V(y) \frac{2Xg(y^2)}{1 + 2Xg(y^2)} dy\right) \quad (10)$$

where

$$V(y) = \frac{30}{y^{12}} - \frac{6}{y^{10}} - \frac{3}{y^8} + \frac{1}{y^6} + \left(-\frac{30}{y^{12}} - \frac{24}{y^{10}} - \frac{6}{y^8} + \frac{1}{4y^4}\right) \exp(-y^2) \quad (11)$$

and the Debye function is given by

$$g(y^2) = \frac{1}{y^2} - \frac{1}{y^4} + \frac{1}{y^4} \exp(-y^2) \quad (12)$$

The integral on the right-hand side of eq 10 can be solved numerically. Now we have the necessary relations for the calculation of η/η_0 . However, as indicated by the empirical eqs 2 and 2a the reduced zero-shear polymer viscosity η_R is a more appropriate quantity for a universal description of the viscosity data. In terms of η_R the model of Shiwa et al. may be cast into the following form:

$$(\eta_R(X))_{S-O-B} = \frac{\alpha r \kappa^2}{\nu x} \quad (13)$$

where

$$\nu = \lim_{X \rightarrow 0} \frac{\eta_{sp}(X)}{X} \quad (14)$$

In the case of excluded-volume interactions a plot of the calculated values (eq 5 combined with eq 10) of η_{sp}/x versus x at small values of x , extrapolated to $x = 0$, yields a value of ν of 0.0719.

Quite recently, Shiwa²² advanced a revised version of the Shiwa et al.¹¹ model by incorporating a modified version of the Hess microscopic theory,¹⁹ in order to take into account the effect of entanglements on the crossover behavior of the polymer viscosity. In an elegant fashion,

Shiwa implemented the entanglement formalism of Hess with the screening concept of Shiwa et al.¹¹ In this framework a unified description of the gradual screening of both hydrodynamic and excluded-volume interactions as well as the effect of entanglements on the polymer viscosity emerges. A formula of the following form may be constructed:^{22,28}

$$(\eta_R)_S = (\eta_R)_{S-O-B}(\eta/\eta_0)_{S-O-B}(1/\mu) \quad (15)$$

or in terms of the other variables used above

$$(\eta_R)_S = \frac{\alpha r \kappa^2}{vX} (1 + \alpha r \kappa^2)(1/\mu) \quad (15a)$$

where the parameter $\mu(X)$ describes the quantitative influence of entanglements on the viscosity process. In the absence of the entanglement effect, μ is put equal to 1. In the presence of entanglements, μ is given by

$$\mu = \begin{cases} 1 - 2E/3 & \text{for } 0 \leq E \leq 1 \\ 1/(1+2E) & \text{for } 1 \leq E \end{cases} \quad (16a)$$

$$(16b)$$

where E is the so-called entanglement parameter. It may be noted that the expression for μ (eq 16) is identical to that which appeared for the reduced self-diffusion coefficient in the original paper¹⁹ of Hess. The quantity E is related to a free-energy density function, representing the excluded-volume interaction contribution to the free-energy density, which may be expressed in terms of the osmotic pressure. By invoking the conformation space RG theory together with the ϵ -expansion method up to order $\epsilon = 4-d$, Oono and Baldwin⁹ derived an explicit functional form, in terms of the overlap parameter X , for the osmotic pressure. In the framework of this model, in the good solvent limit and for a monodisperse sample, the entanglement parameter may be expressed as²⁰

$$E(X) = (1/4) \int_0^X \exp\left\{(\epsilon/4) \left[\left(1 - \frac{1}{X^2}\right) \ln(1+X) + \frac{1}{X} \right] \right\} \quad (17)$$

The integral on the right-hand side of eq 17 has been solved numerically in this study.

In the numerical calculation of E a frequently used augmentation procedure,⁹ which improves the numerical results, has been adopted in this work. The result of this procedure is that the factor $\epsilon/4$ is substituted by $A \equiv (2-d\nu)/(d\nu-1)$ where $d = 3$. The parameter ν is the excluded-volume exponent characterizing the molecular weight dependence of the radius of gyration. For flexible polymers at good solvent conditions, ν assumes a value of 0.588 (the most accurate theoretical value).³³ This yields a value of $A = 0.3089$.

Below some objections to the Shiwa viscosity model, as well as to the approaches which the model is based upon, will be indicated. In the zero-shear viscosity theory of Shiwa,²² the combined mode-coupling/RG model of Shiwa et al.¹¹ is fused with the formalism of Hess,¹⁹ in order to take into account the entanglement effects. Although, consensus seems to exist that the gradual screening of both excluded-volume and hydrodynamic interactions, as well as entanglement effects, is a fundamental cornerstone in a theoretical description of the transport of individual chains in the "effective" semidilute regime, some of the simplifying assumptions and approximations made in the elaboration of the theoretical model discussed here, may be questionable. However, to my knowledge this is the first model which address all these effects in a single model.

In the theory of Shiwa et al., direct interchain interactions are ignored, dynamically, and the excluded-volume interaction enters only through the static correlation functions. This approach does not constitute a unified RG description in the sense that the excluded-volume effects are treated in the framework of the RG concept, whereas the hydrodynamic interactions are considered with the aid of a mode-coupling scheme. It has been argued^{14,34} that the Shiwa et al. model contains a number of uncontrollable approximations. A cornerstone of this model is the inverse of the reduced hydrodynamic screening length κ , which is calculated numerically as a function of the overlap parameter. It is interesting to note that recent sedimentation¹⁶ and diffusion^{17,18} studies, in the framework of a RG model,¹⁰ showed that the values of κ calculated from the Shiwa et al. scheme seem to be consistent with the experimental data.

In the Hess approach a Fokker-Planck equation formalism and projection operator techniques were utilized. In this theory, a Rouse-like behavior is expected to show up at low values of E (eq 16a). When $E \rightarrow 1$, lateral motion is assumed to gradually freeze in, and at larger E values the conjecture is that the motion of a single chain is predominantly governed by curvilinear motion; i.e., a reptation-like stage emerges. The basic hypothesis of the Hess model is that the effects of entanglements are controlled by excluded-volume interactions. Many of the simplifying assumptions and approximations invoked in the theory of Hess have been criticized.^{35,36} A repercussion of these approximations is probably reflected by the peculiar cusplike feature of the theoretical representation, which usually is observed in the transition domain to the reptation-like regime. However, in this context it should be noted that the Hess model, in combination with RG calculations, has been observed to be consistent^{10,20} with experimental self-diffusion and tracer diffusion results.

Finally, we may make some remarks concerning the zero-shear viscosity approach of Shiwa, where the models discussed above are fused together. The description of the transport of individual chains in the semidilute regime constitutes a complicated theoretical problem. In the process of deriving quantities which can directly be compared with experimentally accessible parameters, Shiwa makes a number of simplifying assumptions and approximations. Some of these simplifications may be questionable. The most serious shortcoming is probably that some of the assumptions have been introduced in an ad hoc manner. A challenge for the future is to elaborate a comprehensive theoretical model, which incorporates the effects of excluded-volume interaction, hydrodynamic interactions, and entanglement constraints in a unified way.

Results and Discussion

A principal constituent of the viscosity model discussed above is the static parameter r . In view of the crucial significance of this quantity for the overall success of the viscosity approach it is worthwhile to compare the theoretical predictions with experimental results, e.g., those obtained from small-angle neutron scattering (SANS) experiments. SANS is probably one of the most powerful experimental methods in order to gain insight into this type of problem.

In Figure 1, the ratio $R_{G,c}^2/R_{G,0}^2$ for polystyrene at good solvent conditions is plotted as a function of the experimentally accessible reduced concentration variable X , which may be related^{37,38} to the second virial coefficient A_2 by the following approximate formula: $X = (16/9) -$

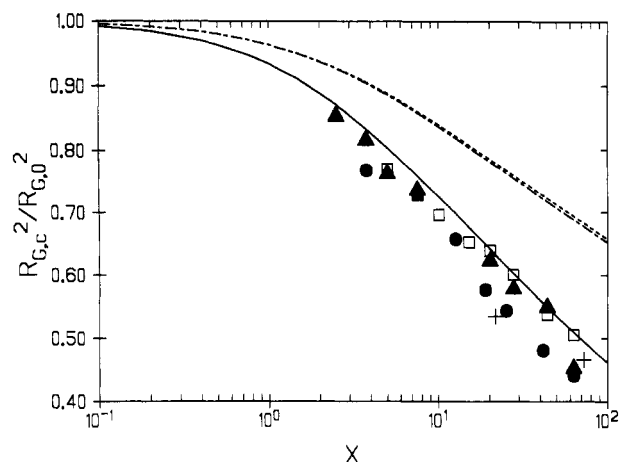


Figure 1. Ratio $R_{G,c}^2/R_{G,0}^2$ for polystyrene systems under good solvent conditions as a function of the scaled static parameter X , which is given by $X = (16/9)A_2Mc$. Polystyrene/carbon disulfide:²⁹ (●) $M = 1.14 \times 10^5$; (+) $M = 5.0 \times 10^5$. Polystyrene/toluene:³¹ (□) $M = 1.14 \times 10^5$ (data of May 1982); (▲) $M = 1.14 \times 10^5$ (data of August 1983). The broken and dot-dashed curves are calculated with the aid of eqs 10 and 7, respectively, by setting $\epsilon = 1$. The solid curve is constructed by using an augmentation procedure where $-\epsilon/4$ in eq 10 is replaced by $2(1-2\nu)/(d\nu-1)$. See text for details.

A_2Mc . This is a dimensionless static scaling parameter. By resorting to this variable, the theoretical curves displayed in Figure 1 have been constructed without introducing any adjustable parameters. Although an extended concentration range is covered in these experiments, we do not believe that the relatively large scatter of the experimental points directly indicates a breakdown^{18,39} of the universality but rather illustrates the magnitude of the experimental errors involved in this type of measurement.^{31,32} In this context it is interesting to note a recent study⁴⁰ of the static and dynamic properties of polymers in a good solvent. By plotting the reduced osmotic pressure as a function of the scaling parameter A_2Mc , a nice condensation of the experimental data was observed. However, if the overlap variable c/c^* was used instead of A_2Mc , a pronounced scatter of the data appeared. This trend was attributed to the greater experimental uncertainty in $R_{G,0}^3$ than in A_2M .

The broken and dot-dashed curves in Figure 1 are calculated with the aid of eqs 10 and 7, respectively, by incorporating the first-order ϵ expansion ($\epsilon = 1$). The numerical results calculated from these two different analytical functions are found to be very close to each other, the deviation between the corresponding r values is at most 1%. However, it is obvious from Figure 1 that these curves, constructed with resort to a first-order ϵ -expansion method, considerably depart from the displayed experimental results. In this connection we may recall that there is a large body of evidence,^{2-5,9,16-18,20} indicating that the quantitative agreement between theoretical predictions and experimental data may be improved significantly if an adequate augmentation procedure is fused with the RG results. In order to recover the correct scaling behavior in the asymptotic limit and to account partially for the higher-order correction of ϵ , Ohta and Nakanishi argued² for an augmentation scheme where the factor $-\epsilon/4$ in eq 10 is replaced by $2(1-2\nu)/(d\nu-1)$ with $d = 3$ and $\nu = 0.588$. The solid curve in Figure 1 is constructed with the aid of this procedure, and in this case the accordance between the theoretical description and the experimental data is reasonably good. This finding calls into question the reliability of the first-order ϵ -expansion method in providing sufficiently accurate nu-

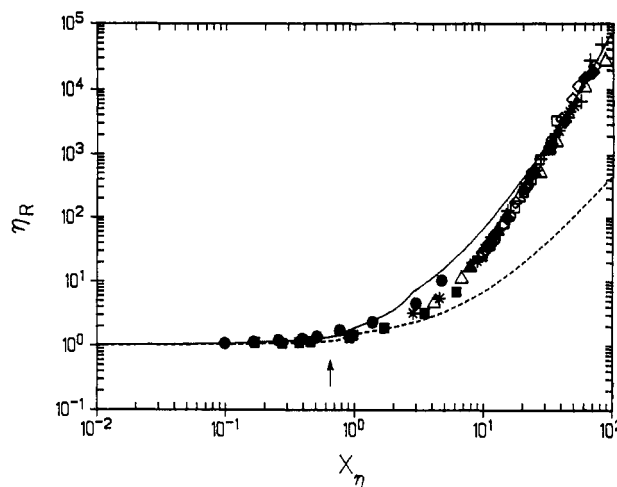


Figure 2. Reduced zero-shear viscosity for polystyrene under good solvent conditions as a function of the scaled dynamic variable X_η , which is related to $[\eta]$ by $X_\eta = 0.67c[\eta]$. Polystyrene/toluene:²⁴ (●) $M = 5.1 \times 10^4$; (■) $M = 1.8 \times 10^5$. Polystyrene/benzene:⁵⁸ (▲) $M = 3.8 \times 10^5$; (*) $M = 6.8 \times 10^5$; (Δ) $M = 20.6 \times 10^5$. Polystyrene/ α -chloronaphthalene:²⁶ (□) $M = 7.8 \times 10^5$; (○) $M = 1.3 \times 10^6$; (◇) $M = 4.5 \times 10^6$; (+) $M = 8.4 \times 10^6$; (◆) $M = 20.6 \times 10^6$. The broken curve represents eq 15a with $\mu = 1$ (in absence of entanglements). The solid curve is calculated by means of eq 15a in combination with eqs 16 and 17 (entanglements are accounted for). The vertical arrow indicates transition to the semidilute regime.

merical results. In view of this, augmentation is also resorted to, in this study, in the calculation of numerical results related to the viscosity models. In this context it should be mentioned that in principle an augmentation scheme similar to that above should be employed in connection with eq 5a. However, to our knowledge a convenient augmentation procedure to replace $-31\epsilon/96 + \gamma\epsilon/8$ does not exist.

Figure 2 shows a log-log representation of the reduced zero-shear polymer viscosity versus the dynamic scaling function X_η for polystyrene at good solvent conditions. In order to establish a functional form between the overlap parameter X and the dimensionless dynamic counterpart $c[\eta]$, inherent scaling variable in the analysis of the viscosity results, a numerical identification procedure between the empirical relation eq 2 and eq 15 is carried out at low values of X . In this process a value of k_H of 0.38 is employed. This theoretical value was devised by Muthukumar and Freed⁴¹ in the framework of a generalized version of the Freed-Edwards theory of the concentration dependence of the hydrodynamics of a polymer solution to consider the Huggins coefficient for polymers with fully developed excluded-volume interactions. This value of k_H is in accord with experimental values observed⁴²⁻⁴⁴ for polystyrene in good solvents. Furthermore, the cited investigations also indicate that k_H is practically independent of M over an extended range ($5 \times 10^4 < M < 6 \times 10^7$), but k_H increases as the solvent power decreases. The following relationship emerges from this comparison procedure $X_\eta = 0.67c[\eta]$. The data in Figure 2 are plotted by utilizing this relation together with the expression $[\eta]$ (cm³/g) = $9.06 \times 10^{-3}M^{0.74}$ reported⁴⁵ for polystyrene at good solvent conditions. The universality of the plot is illustrated by the good condensation of the experimental points. In passing by, it may be noted that in a previous study⁴⁶ it was shown that the viscosity data for polystyrene samples with a broad molecular weight distribution condensed on the same curve (η_R versus $c[\eta]$) as the data for the monodisperse fractions, if the polydispersity effects were accounted for.

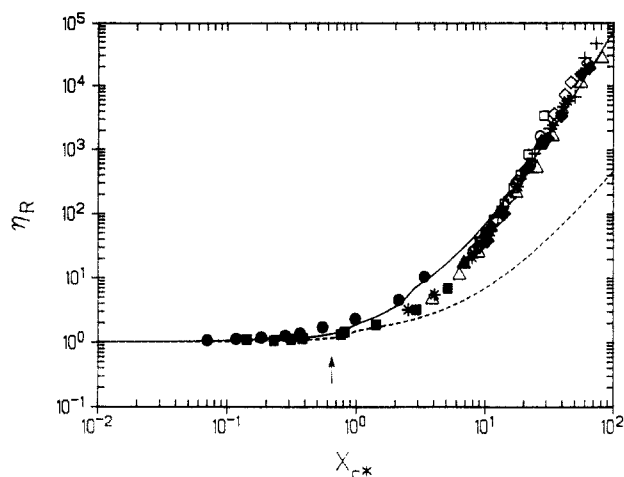


Figure 3. Reduced zero-shear viscosity for polystyrene under good solvent conditions as a function of the scaled static variable X_{c^*} , which is related to c^* by $X_{c^*} = 0.65(c/c^*)$. Symbols are the same as in Figure 2. The broken curve represents eq 15a with $\mu = 1$ (in the absence of entanglements). The solid curve is constructed from eq 15a in combination with eqs 16 and 17 (entanglements are accounted for). The vertical arrow indicates transition to the semidilute regime.

The broken curve in Figure 2, constructed from eq 15a with $\mu = 1$ (effects of entanglement are neglected), exhibits a progressive departure from the experimental data in the semidilute regime. This tendency probably reflects that entanglements have a crucial influence on the viscosity process of long polymer chains in the semidilute range. The solid curve, determined by means of eq 15a in combination with eqs 16 and 17, represents a situation where the entanglement effects have been accounted for. In this case the experimental data are in a broad outline described by the theoretical model. An inspection of Figure 2 reveals a peculiar shape of the theoretical curve in the transition ($E \rightarrow 1$) to reptation-like behavior. As was mentioned above, this effect is attributed¹⁹ to an artifact of the approximation made in the entanglement model of Hess.

Figure 3 shows a comparison of the same experimental data as in Figure 2 with the same theoretical predictions as before, but here η_R is plotted versus X_{c^*} (the radius of gyration is determined from $R_{G,0}^2 (\text{cm}^2) = 1.38 \times 10^{-18} M^{1.19}$ reported⁴⁵ for polystyrene at good solvent conditions), where $X_{c^*} = 0.65(c/c^*)$. This relationship is obtained through a numerical identification procedure analogous to that described above, but in this case eq 15a is compared with eq 2a and k_H and Ψ are put equal to 0.38 and $1.67 \times 10^{23} (\text{mol}^{-1})$, respectively. The value of the Flory-Fox parameter has been determined for nondraining self-avoiding chains by Oono and Kohmoto⁴⁷ with the aid of RG theory together with the first-order ϵ -expansion calculation. The main features in Figure 3 are similar to those depicted in Figure 2. However, a thorough comparison of the data in Figure 2 and 3 reveals a somewhat larger scatter of the experimental points in the latter figure. Below some of the possible sources which may give rise to the observed scatter are scrutinized.

It should be noticed that the parameters $c[\eta]$ and c/c^* both represent a measure of the degree of coil overlapping. However, the former quantity may be viewed as a dynamic scaling variable, whereas the latter, in the way it is defined here (see eq 3), constitutes a static overlap parameter. It has previously been observed^{9,38,48} that a static scaling variable often fails to condense data obtained from dynamic experiments in a universal manner. In view of this and the somewhat larger scatter of the experimental

points in Figure 3 as compared with Figure 2, it may be instructive to consider some of the approximations involved by using the scaling variable c/c^* instead of $c[\eta]$.

In the transformation of $c[\eta]$ into c/c^* the Flory-Fox theory ($[\eta] \propto R_{G,0}^3/M$) is frequently used. However, theoretical advances due to Weill and des Cloizeaux suggest⁴⁹ that $[\eta] \propto R_{G,0}^2 R_H/M$, where R_H is the hydrodynamic radius of the isolated polymer is a more correct representation of the intrinsic viscosity. At good solvent conditions, both the blob^{49,50} theory and RG calculations⁵¹ show that R_H reaches its asymptotic behavior more slowly than $R_{G,0}$, and extremely long polymer chains are needed in order to realize this limit for dynamic properties. This prediction is in qualitative agreement with experimental results.⁵²

The factor Ψ plays an important role in the Flory-Fox model as well as in the transformation from $c[\eta]$ to c/c^* . For polystyrene at good solvent conditions it has been found experimentally^{44,53} that Ψ decreases slowly ($\Psi \propto M^{-0.05}$) with increasing molecular weight. Polydispersity effects^{54,55} are another factor which may affect the value of Ψ . Furthermore, the influence of effects such as draining and excluded volume may come into play and should be assessed. Quite recently, it was argued⁵⁶ that Ψ is nonuniversal even in the nondraining limit at good solvent conditions. There are also other aspects which should be considered in the process of selecting the most adequate scaling variable for the analysis of viscosity data. It has been claimed³⁸ that when c^* is expressed in terms of $M/R_{G,0}^3 N_A$, this choice poses several practical problems, because the result obtained for c^* for a sample with even moderate polydispersity is very sensitive to the type of averaging involved (for example, number, weight, or z average). In addition, it may be expected that the experimental uncertainty in $M/R_{G,0}^3$ is greater than that in $[\eta]$. It has been observed⁴⁴ that zero-shear-rate intrinsic viscosity data of polystyrene in good solvents can be described accurately by a single Mark-Houwink-Sakurada relation over an extended molecular weight range. Finally, it should be noticed that the definition of c^* does not provide a unique quantity which unambiguously marks the demarcation between the dilute and the semidilute regimes. The definition of c^* is rather arbitrary and only roughly indicates the transition from dilute to semidilute solution behavior.⁵⁷ Moreover, the value of c^* seems to be correlated to the type of physical phenomena investigated. For instance, it has been observed²⁷ that the crossover concentration, separating the dilute from the semidilute regime, is about 5 times higher for zero-shear viscosity than the corresponding one for thermodynamic properties. In light of the arguments presented above it may be concluded that $c[\eta]$ constitutes a more adequate and natural scaling variable than c/c^* in the analysis of universal zero-shear viscosity properties.

Before we proceed, it is relevant to make some comments concerning the reason for the apparent different appearance of the experimental data in Figure 3 as compared with an analogous plot displayed in the paper²² of Shiwa. In the cited work it has been observed that the experimental data from two different research groups are widely separated from each other. One group (Takahashi et al.²⁶) determined the values of c^* for the system polystyrene/ α -chloronaphthalene by using eq 3 together with the relation $R_{G,0}^2 (\text{cm}^2) = 1.38 \times 10^{-18} M^{1.19}$, which has been found to hold for solutions of polystyrene at good solvent conditions. The other group (Adam and Delsanti⁵⁸) utilized an overlap concentration defined by $c^* = M/R_{G,0}^3 N_A$, and the values of $R_{G,0}$ were calculated from^{59,60}

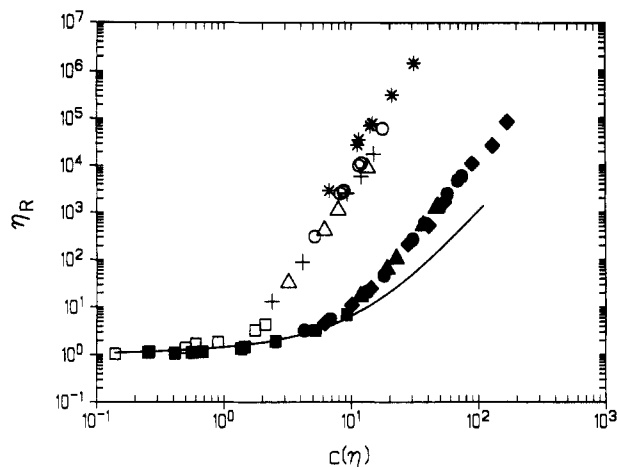


Figure 4. Reduced zero-shear viscosity for polystyrene under good and Θ solvent conditions as a function of the scaled dynamic parameter $c[\eta]$. Polystyrene/toluene:²⁴ (■) $M = 1.8 \times 10^6$. Polystyrene/benzene:⁵⁸ (▲) $M = 3.8 \times 10^6$; (●) $M = 6.8 \times 10^6$; (◆) $M = 20.6 \times 10^6$. Polystyrene/cyclohexane:^{24,68,69} (□) $M = 1.50 \times 10^6$; (Δ) $M = 3.8 \times 10^6$; (○) $M = 6.8 \times 10^6$; (+) $M = 7.1 \times 10^6$; (*) $M = 20.6 \times 10^6$. The solid curve is constructed with the aid of eq 15a ($r = 1$, $\alpha = 1$, and $\mu = 1$) in combination with eq 6. Entanglement effects are not taken into account. See text for details.

$R_{G,0}^2$ (cm^2) = $2.10 \times 10^{-18} M^{1.19}$. In the present study the ratio c/c^* was determined with the aid of the former relationship for all the polystyrene-solvent pairs at good solvent conditions. However, in the work of Shiwa the values of c^* reported by the two different groups were used,²⁸ and the values of c^* used by Adam and Delsanti were transformed to the overlap concentration defined by eq 3. It is easy to see that the above relationships for the calculation of the radius of gyration yield different values of $R_{G,0}$. Consequently, the values of c/c^* ($c^* \sim 1/R_{G,0}^3$) for the two systems will differ significantly and the separation effect observed by Shiwa is expected. In the examination of these features we have found that the relation used by Adam and Delsanti in the evaluation of $R_{G,0}$ for the system polystyrene/benzene is not compatible with the results published in the literature^{61,62} for the same system. The expression utilized by Adam and Delsanti yields values of $R_{G,0}$ which are about 20% larger than those inferred from the literature. It should also be noted that the values of $R_{G,0}$ calculated from ref 62 are consistent with those determined from the relationship used in the present investigation. These findings indicate that the separation of the data sets observed in the paper²² of Shiwa is simply due to erroneous values of c/c^* for the system polystyrene/benzene.

In Figure 4 experimental viscosity data of polystyrene over wide ranges of molecular weight and concentration, and at both good and Θ solvent conditions, are depicted on a log-log plot of the form η_R versus $c[\eta]$. The solid curve represents polymer solutions at Θ solvent conditions and has been constructed with the aid of eq 15a ($r = 1$, $\alpha = 1$, and $\mu = 1$) in combination with eq 6. An identification procedure similar to that used before yields the following relationship: $X_{\eta}^{\Theta} = 0.40c[\eta]$. In this evaluation a value of $k_H = 0.76$, derived from the theory of Freed and Edwards⁶³ for solutions of Gaussian random-coil chains, was used. Since $c[\eta]$ is utilized as a scaling variable, the numerical results are adjusted in order to conform to this parameter.

Let us first compare the results at good and Θ solvent conditions. A conspicuous feature is the much stronger increase of η_R with the overlap parameter for the Θ system than for polystyrene in a good solvent. A plausible

explanation of this effect is that the strength of the entanglement⁶⁴ is more pronounced when the solvent power diminishes. In order to further consolidate this conjecture and to elucidate this phenomenon from another angle of approach, some recent results obtained from measurements with a different experimental technique may be quoted.

In a recent dynamic light scattering study⁶⁵ on the system polystyrene/*trans*-decalin in the semidilute regime, measurements were carried out at various temperatures in the region from the upper critical solution temperature (UCST) to moderately good solvent conditions. The resulting time correlation functions of concentration fluctuations are very well described by a single exponential (at short times) followed by a nonexponential relaxation function, which is characterized by a fractional exponential of the William-Watts type. The mean relaxation time, evaluated at long times, was found to increase with decreasing solvent power; the increase was observed to be especially strong in the vicinity of the UCST. Since the long-time-scale behavior is considered to be related to the topological interaction, this finding endorses the hypothesis of enhanced effects of entanglement as the thermodynamic conditions become poorer.

In the comparison of the viscosity results in Figure 4, the data at the Θ point apparently exhibit a much larger scatter than those at good solvent conditions. However, this impression is essentially due to the systematic and significant deviation toward higher values of η_R displayed by the data representing the highest molecular weight ($M = 20.6 \times 10^6$). It is well-known^{66,67} that for very long polymer chains immersed in a Θ solvent the Θ temperature practically coincides with the critical solution temperature. This suggests that the Θ temperature for the highest molecular weight sample is close to the experimental cloud-point curve and hence the solvent at Θ should be a poor solvent. This may give rise to enhanced entanglement effects in solutions of the highest molecular weight. In this connection, it is interesting to note the results of a previous paper,²⁶ where the reduced zero-shear viscosity for polystyrene ($4.5 \times 10^6 \leq M \leq 20.6 \times 10^6$) in dioctyl phthalate was measured over an extended concentration region. Although the measurements were performed at 30 °C instead of 22 °C (the Θ point for this polymer-solvent pair), this system was considered to exhibit approximate Θ behavior. However, in contrast to the polystyrene/cyclohexane system, all data, even those representing the highest molecular weight, collapsed onto a single curve. This may support the above conjecture that the observed departure of the data of the highest molecular weight sample originates from effects appearing close to the cloud-point curve. Another feature which is visible on comparison of the data in Figure 4 is that the domain between the dilute and semidilute regimes is much smaller at the Θ state than at good solvent conditions.

It is obvious from Figure 4 that the theoretical prediction, constructed for Gaussian chains with no entanglement effects, for the reduced zero-shear viscosity, is only capable of depicting the experimental behavior at low values of $c[\eta]$ (up to $c[\eta] \approx 1$); above this value a gradual increasing departure from the experimental data is observed. This finding corroborates with the assertion that entanglements constitute a crucial feature in the understanding of viscosity properties of long-chain molecules in the semidilute region. Unfortunately, there is no microscopic theory available at present which incorporates, in the form of an explicit function, entanglement effects at Θ solvent conditions.

Conclusions

In this study reduced zero-shear viscosity data, collected from the literature, for polystyrene in the dilute and the effective semidilute ranges and at good and θ solvent conditions, are compared with recent theoretical predictions. At good solvent conditions, the behavior of the ratio $R_{G,c^2}/R_{G,0}^2$ as a function of the matrix concentration, expressed in terms of an experimentally accessible reduced concentration variable, plays a central role for the outcome of the approach. If a convenient augmentation procedure is adopted in lieu of setting $\epsilon = 1$, a reasonably good agreement between the theoretical prediction and the experimental results is obtained.

The universality of zero-shear polymer viscosity properties has been confirmed by plotting a large amount of experimental viscosity data on the form η_R versus an overlap parameter. A somewhat better condensation of the data is observed by utilizing the dynamic scaling variable $c[\eta]$ instead of the static counterpart c/c^* . A number of arguments are presented in favor of the use of $c[\eta]$ as a scaling variable instead of c/c^* in the analysis of the viscosity results. At good solvent conditions a reasonably good accordance between the experimental data and the theoretical prediction is found when the gradual screening of both hydrodynamic and excluded-volume interactions as well as entanglement effects in the semidilute regime is taken into account.

Due to the lack of an appropriate model to incorporate entanglement effects in the semidilute θ regime, the approach used here is only capable of depicting the viscosity behavior in the dilute range. Entanglements are found to play a crucial role for the viscosity process in the semidilute regime at all thermodynamic conditions. However, the strength of the entanglement constraint seems to increase as the solvent power decreases.

The apparent breakdown of the universality of the reduced zero-shear viscosity observed for the highest molecular weight sample in the semidilute θ region is attributed to the close proximity of the concentrations of this molecular weight to the cloud-point curve.

Acknowledgment. The author thanks Professor Y. Shiwa for helpful correspondences.

References and Notes

- Ohta, T.; Oono, Y. *Phys. Lett.* **1982**, *89A*, 460.
- Ohta, T.; Nakanishi, A. *J. Phys. A* **1983**, *16*, 4155.
- Nakanishi, A.; Ohta, T. *J. Phys. A* **1985**, *18*, 127.
- Oono, Y. *Adv. Chem. Phys.* **1985**, *61*, 301.
- Cherayil, B. J.; Bawendi, M. G.; Miyake, A.; Freed, K. F. *Macromolecules* **1986**, *19*, 2770.
- Freed, K. F. *Renormalization Group Theory of Macromolecules*; Wiley-Interscience: New York, 1987.
- Jannink, G.; des Cloizeaux, J. *J. Phys.: Condens. Matter* **1990**, *2*, 1.
- des Cloizeaux, J.; Jannink, G. *Polymers In Solution: Their Modelling and Structure*; Oxford University Press: Oxford, U.K., 1990.
- Oono, Y.; Baldwin, P. R. *Phys. Rev. A* **1986**, *33*, 3391.
- Shiwa, Y. *Phys. Rev. Lett.* **1987**, *58*, 2102.
- Shiwa, Y.; Oono, Y.; Baldwin, P. R. *Macromolecules* **1988**, *21*, 208.
- Shiwa, Y. *J. Phys. A* **1991**, *24*, L-579.
- Doi, M.; Edwards, S. F. *The Theory of Polymer Dynamics*; Oxford University Press: Oxford, U.K., 1986.
- Fredrickson, G. H.; Helfand, E. *J. Chem. Phys.* **1990**, *93*, 2048.
- Nyström, B.; Waernes, O.; Roots, J. *J. Polym. Sci., Polym. Lett. Ed.* **1989**, *27*, 271.
- Nyström, B.; Roots, J. *J. Polym. Sci., Polym. Phys. Ed.* **1990**, *28*, 521.
- Nyström, B.; Roots, J. *J. Polym. Sci., Polym. Lett. Ed.* **1990**, *28*, 101.
- Nyström, B.; Roots, J. *Polymer* **1992**, *33*, 1548.
- Hess, W. *Macromolecules* **1986**, *19*, 1395.
- Nyström, B.; Roots, J. *Macromolecules* **1991**, *24*, 184.
- Stepanow, S.; Helms, G. *Macromolecules* **1991**, *24*, 1408.
- Shiwa, Y. *J. Phys. II, Fr.* **1991**, *1*, 1331.
- Dreval, V. E.; Malkin, A. Y.; Botvinnik, G. O. *J. Polym. Sci., Polym. Phys. Ed.* **1973**, *11*, 1055.
- Zakin, J. L.; Wu, R.; Luh, H.; Mayhan, K. G. *J. Polym. Sci., Polym. Phys. Ed.* **1976**, *14*, 299.
- Takahashi, Y.; Isono, Y.; Noda, I.; Nagasawa, M. *Macromolecules* **1985**, *18*, 1002.
- Takahashi, Y.; Noda, I.; Nagasawa, M. *Macromolecules* **1985**, *18*, 2220.
- Noda, I. In *Molecular Conformation and Dynamics of Macromolecules in Condensed Systems*; Nagasawa, M., Ed.; Elsevier: Amsterdam, The Netherlands, 1988; p 85.
- Shiwa, Y., private communication.
- Daoud, M.; Cotton, J. P.; Farnoux, B.; Jannink, G.; Sarma, G.; Benoit, H.; Duplessix, R. Picot, C.; de Gennes, P.-G. *Macromolecules* **1975**, *8*, 804.
- Hayashi, H.; Hammada, F.; Nakajima, A. *Makromol. Chem.* **1977**, *178*, 827.
- King, J. S.; Boyer, W.; Wignall, G. D.; Ullman, R. *Macromolecules* **1985**, *18*, 709.
- Wignall, G. D. *Encycl. Polym. Sci. Eng.* **1987**, *10*, 112.
- Le Guillou, J. C.; Zinn-Justin, J. *Phys. Rev. Lett.* **1977**, *39*, 95.
- Muthukumar, M. *Macromolecules* **1988**, *21*, 2891. See Also: Shiwa, Y.; Oono, Y. *Macromolecules* **1988**, *21*, 2892.
- Schweizer, K. S. *J. Chem. Phys.* **1989**, *91*, 5802; **1989**, *91*, 5822.
- Skolnick, J.; Kolinski, A. *Adv. Chem. Phys.* **1990**, *78*, 223.
- Wiltzius, P.; Haller, H. R.; Cannell, D. S.; Schaefer, D. W. *Phys. Rev. Lett.* **1983**, *51*, 1183.
- Cannell, D. S.; Wiltzius, P.; Schaefer, D. W. In *Physics of Complex and Supermolecular Fluids*; Safran, S. A., Clark, N. A., Eds.; Wiley: New York, 1987; p 267.
- Shiwa, Y.; Oono, Y.; Baldwin, P. R. *Mod. Phys. Lett. B* **1990**, *4*, 1421.
- Adam, M.; Fetters, L. J.; Graessley, W. W.; Witten, T. A. *Macromolecules* **1991**, *24*, 2434.
- Muthukumar, M.; Freed, K. F. *Macromolecules* **1977**, *10*, 899.
- Sakato, K.; Kurata, M. *Polym. J. (Jpn.)* **1970**, *1*, 260.
- Bohdanecky, M. *Collect. Czech. Chem. Commun.* **1970**, *35*, 1972.
- Einaga, Y.; Miyaki, Y.; Fujita, H. *J. Polym. Sci., Polym. Phys. Ed.* **1979**, *17*, 2103.
- Noda, I.; Higo, Y.; Ueno, N.; Fujimoto, T. *Macromolecules* **1984**, *17*, 1055.
- Takahashi, Y.; Sakakura, D.; Wakutsu, M.; Yamaguchi, M.; Noda, I. *Polym. J. (Jpn.)* **1992**, *24*, 987.
- Oono, Y.; Kohmoto, M. *J. Chem. Phys.* **1983**, *78*, 520.
- Wiltzius, P.; Haller, H. R.; Cannell, D. S.; Schaefer, D. W. *Phys. Rev. Lett.* **1984**, *53*, 834.
- Weill, G.; des Cloizeaux, J. *J. Phys. (Paris)* **1979**, *40*, 99.
- Akcasu, A. Z.; Han, C. C. *Macromolecules* **1979**, *12*, 276.
- Oono, Y. *J. Chem. Phys.* **1983**, *79*, 4629.
- Wolinski, L.; Witkowski, K.; Turzynski, Z.; Szafko, J. *J. Polym. Sci., Polym. Phys. Ed.* **1990**, *28*, 811.
- Varma, B. K.; Fujita, Y.; Takahashi, M.; Nose, T. *J. Polym. Sci. Polym. Phys. Ed.* **1984**, *22*, 1781.
- Douglas, J. F.; Freed, K. F. *J. Chem. Phys.* **1984**, *88*, 6613.
- Konishi, T.; Yoshizaki, T.; Yamakawa, H. *Macromolecules* **1991**, *24*, 5614.
- Shiwa, Y.; Oono, Y. *Physica A* **1991**, *174*, 223.
- Nyström, B.; Roots, J. *Prog. Polym. Sci.* **1982**, *8*, 333.
- Adam, M.; Delsanti, M. *J. Phys. (Paris)* **1983**, *44*, 1185.
- Decker, D. Thesis, Strasbourg, France, 1968.
- Adam, M.; Delsanti, M. *Macromolecules* **1977**, *10*, 1229.
- Fukuda, M.; Fukutomi, M.; Kato, Y.; Hashimoto, T. *J. Polym. Sci., Polym. Phys. Ed.* **1974**, *12*, 871.
- Miyaki, Y.; Einaga, Y.; Fujita, H. *Macromolecules* **1978**, *11*, 1180.
- Freed, K. F.; Edwards, S. F. *J. Chem. Phys.* **1975**, *62*, 4032.
- Isono, Y.; Nagasawa, M. *Macromolecules* **1980**, *13*, 862.
- Nyström, B.; Roots, J. *Macromolecules*, submitted for publication.
- Flory, P. J. *Principles of Polymer Chemistry*; Cornell University Press: Ithaca, NY, 1953.
- Kurata, M. *Thermodynamics of Polymer Solutions*; Harwood Academic Publishers: New York, 1982.
- Adam, M.; Delsanti, M. *J. Phys. (Paris)* **1984**, *45*, 1513.
- Adam, M.; Delsanti, M. *J. Phys. (Paris)* **1982**, *43*, 549.